HydroLight Technical Note 12

Sky Radiance Effects

Curtis Mobley

April 22, 2016

Beginning with version 5.3, HydroLight has an option to input user-defined files containing measured or modeled sky radiances $L_{\rm sky}(\theta, \phi, \lambda)$. If this is done, the sky radiance is provided by the user, and the default HydroLight sky irradiance and radiance submodels are not needed. Inputting a user-defined $L_{\rm sky}(\theta, \phi, \lambda)$ gives several improvements to HydroLight simulations:

- The angular pattern of the sky radiance can depend on wavelength.
- Arbitrary sky radiance distributions (e.g., to included the effects of non-uniform cloud distributions) can be incorporated in the the HydroLight computations.
- HydroLight can be run for any wavelengths for which the sky radiance is input, *so long as the inherent optical properties (IOPs) and other inputs are known over the same range of wavelengths*.

This note discusses when the use of a more accurate sky radiance is justified, and when it is unnecessary. The sensitivities of in-water radiances and apparent optical properties (AOPs) to the magnitude and angular distribution of the sky radiance $L_{\rm sky}(\theta, \phi, \lambda)$ are illustrated. The conclusion is that the default sky irradiance and radiance models in HydroLight are adequate for the study of AOPs such as the remote-sensing reflectance $R_{\rm rs}$ or diffuse attenuation $K_{\rm d}$. However, if performing a closure experiment in which in-water radiances in particular directions are compared with measured radiances, then the use of a sky radiance distribution measured at the time of the experiment is warranted.

The default in HydroLight is to model the sky radiance incident onto the sea surface by combining a model for the spectral sky irradiance with a model for the angular distribution of the sky radiance. The direct (transmitted solar beam) and diffuse (background sky) irradiances incident onto the sea surface are obtained from the RADTRAN clear-sky irradiance model of Gregg and Carder (1990), as extended from 700 to 1000 nm and from 350 to 300 nm, and as scaled for cloud cover by the model of Kasten and Czeplak (1980). This extended RADTRAN model (called RADTRAN-X) is discussed in HydroLight Technical Note 4. The angular pattern of the sky radiance, normalized to the sun's direction, is given by the semi-analytical model of Harrison and Coombes (1988). That model is based on broad-band observations of clear and cloudy skies over the wave length range from 300 to 3000 nm and includes a cloud-fraction parameter. The normalized angular pattern is re-scaled at each wavelength so that the integral over direction of the sky radiance distribution gives the spectral irradiance value of Gregg and Carder (1990). These models have proven sufficiently accurate for most HydroLight applications.

However, one disadvantage of using the RADTRAN-X model is that its underlying database covers only the 300-1000 nm range. Consequently, HydroLight can be run only from 300 to 1000 nm. In addition, the angular pattern of the sky radiance does not depend on wavelength because the Harrison and Coombes model is a best fit to broad-band measurements. In reality, the angular pattern of the clear-sky radiance does depend on wavelength because the relative contributions of Rayleigh and aerosol scattering to the total diffuse sky radiance change with wavelength. Moreover, the Harrison and Coombes angular distribution is symmetric about the solar plane, so that the effects of individual clouds cannot be modeled; the effects of individual clouds can make the radiance distribution highly asymmetric. Important warnings are given on running HydroLight outside the 300 to 1000 nm range for which the underlying databases of inherent optical properties, bottom reflectances, and other inputs are available.

Example Sky Radiance Distribution

To generate an example realistic sky radiance distribution for use in HydroLight, the MODTRAN atmospheric radiative transfer model (Berk et al., 2000) was used as follows:

- The Sun zenith angle was $\theta_{\rm Sun} = 60$ deg and the Sun's azimuthal angle was at $\phi_{\rm Sun} = 0$, where $\phi = 0$ is the downwind direction in HydroLight.
- The atmospheric conditions (temperature profile, water vapor, ozone, etc.) were typical of a tropical marine atmosphere (defined via MODTRAN's "Tropical Atmosphere" option). The sky conditions were clear. The aerosols were for an open-ocean marine atmosphere.
- The wind speed was 10 m $\rm s^{-1}$.
- The wavelength resolution was 10 nm from 350 to 1500 nm.

A single MODTRAN run can generate the radiance at all requested wavelengths for a particular sky viewing direction (θ_v, ϕ_v). Code was written to loop over the grid of (θ_v, ϕ_v) values for the HydroLight quad centers, which are at

- $\theta_v = 0 \text{ (polar cap)}, 10, 20, 30, 40, 50, 60, 70, 80, 87.5$ deg
- $\phi_v = 0, 15, 30, ..., 345$ deg

The resulting MODTRAN-computed sky radiances were collected in a file on the HydroLight Standard Format for sky radiance distributions. That format is described in the H5.3 Technical Documentation.

The left panel of Fig. 1 shows the MODTRAN-computed radiances in the plane of the sun at selected wavelengths. Positive θ_v values are in the half plane looking toward the sun ($\phi_v = 0$), and negative θ_v values are in the half plane facing away from the sun ($\phi_v = 180$ deg). The right panel shows the radiances normalized to the maximum value in the direction of the sun at $\theta_v = 60$ deg. The black line in that panel shows the shape of the radiance distribution as given by the semi-analytic model of Harrison and Coombes (1988). The shape of the radiance distribution clearly depends on wavelength, and the Harrison and Coombes model can be off by more than an order of magnitude in directions away from the sun. The primary question to be addressed in this note is then, "How important are these differences in the shape of the radiance distribution?"

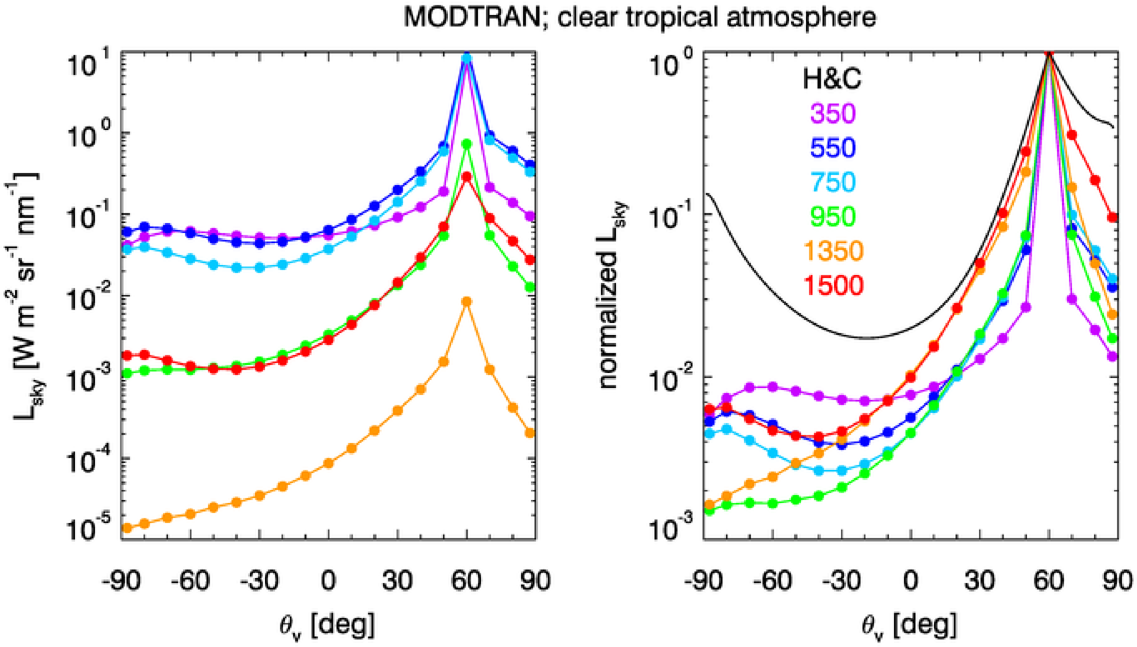

Figure 1: Example MODTRAN-computed sky radiances in the plane of the sun. Left panel: radiances at selected wavelengths. Right panel: radiances normalized to their maximum values in the direction of the sun. The black line is the shape of the radiance as given by the model of Harrison and Coombes (1988).

Quad-Averaged Radiances vs. Quad-Center Radiances

There are two options for how a file of user-defined sky radiances is processed in HydroLight v 5.3. The first, which is the recommended option, is to input a file of quad-averaged $L_{\text{sky}}(\theta, \phi, \lambda)$ values. This requires that the (θ, ϕ) values in the input file correspond exactly to the HydroLight standard quad partition, whose quad centers are listed above. This option gives the user the ability to compute the quad-averages sky radiances exactly as desired (e.g., by high-angular-resolution integrations over the HydroLight quads).

The second option is to treat the $L_{\text{sky}}(\theta, \phi, \lambda)$ values as radiances in the exact directions of the (θ, ϕ) values in the input file. HydroLight then interpolates between these values to compute the needed quad averages. With this option, the values at each direction can influence the quad averages for the neighboring quads. This is illustrated in Fig. 2. The solid blue lines represent a 3×3 block of θ-ϕ quads. The solid red dots represent the $L_{\text{sky}}(\theta, \phi, \lambda)$ data values, taken to be at the quad centers. The default in HydroLight is to divide each quad into a 3×5 set of subquads, which gives roughly 3 deg × 3 deg subquads for the standard 10 deg × 15 deg θ-ϕ quads. The subquads

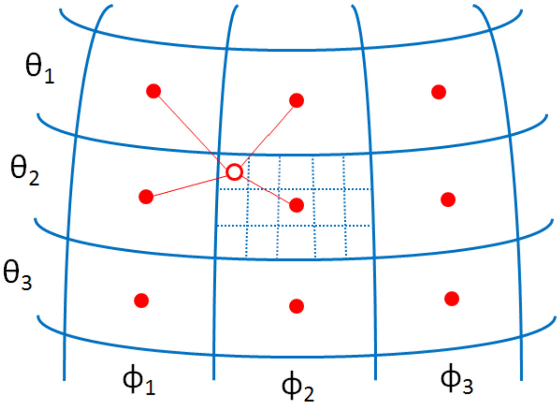

Figure 2: Illustration of interpolation of sky radiance values when the values are treated as radiances in particular directions.

for quad centered at θ_2, ϕ_2 are shown by the blue dotted lines. When computing quad-averaged sky radiances using the formalism of *Light and Water* (Mobley, 1994) Eqs. (4.64) and (8.13), the radiance must be known at the center of each subquad. One of these needed values is illustrated by the open red circle. The sky radiance value at that point is obtained by bi-linear interpolation from the nearest points for which the radiance is known. For the open circle, the nearest points are shown by the red lines.

The effect of this interpolation is illustrated in Fig. 3. The red circles are the MODTRAN values in the input file processed as quad-averaged radiances. The blue dots are the same input data, but used as quad-center values, with bi-linear interpolation in θ, ϕ space used to compute the quad averages. The left panel shows that the quad with the sun has a smaller quad-averaged value when that quad's center value is averaged with the darker neighboring points to get a quad average. The right panel shows that the neighboring quads in the ϕ = 15-195 plane are increased by the brighter solar quad (at $\phi = 0$) when interpolation is used.

Strictly speaking, these two options for processing sky radiance data give two different sets of quad-averaged sky radiances, hence two different solutions of the radiative transfer equation (RTE). However, the differences in the computed radiance distributions are negligible for many purposes, especially for computation of AOPs, as seen in Figs. 5-7 below.

MODTRAN vs. RADTRAN plus Harrison and Coombes

A HydroLight run was made using the default RADTRAN-X model to compute the sky irradiances and Harrison and Coombes to define the angular shape of the sky radiance distribution. The sun was again at $(\theta_{\rm Sun}, \phi_{\rm Sun}) = (60, 0)$. The RADTRAN atmospheric conditions were for a clear sky and marine aerosols. However, it is not possible to exactly match the atmospheric conditions used for the MODTRAN run because the two codes have different inputs. Therefore, the computed sky irradiances will be somewhat different because the two atmospheres are different. Figure 4 shows the total (sun plus sky) irradiances $E_d(\lambda)$ incident onto the sea surface as computed by RADTRAN and by MODTRAN. The two irradiance spectra differ by up to 30% in the 350-800 nm range. These differences in sky irradiances carry through to the RTE solution and will correspondingly affect the in-water radiance and irradiance magnitudes. AOPs, however, are very insensitive to magnitude effects.

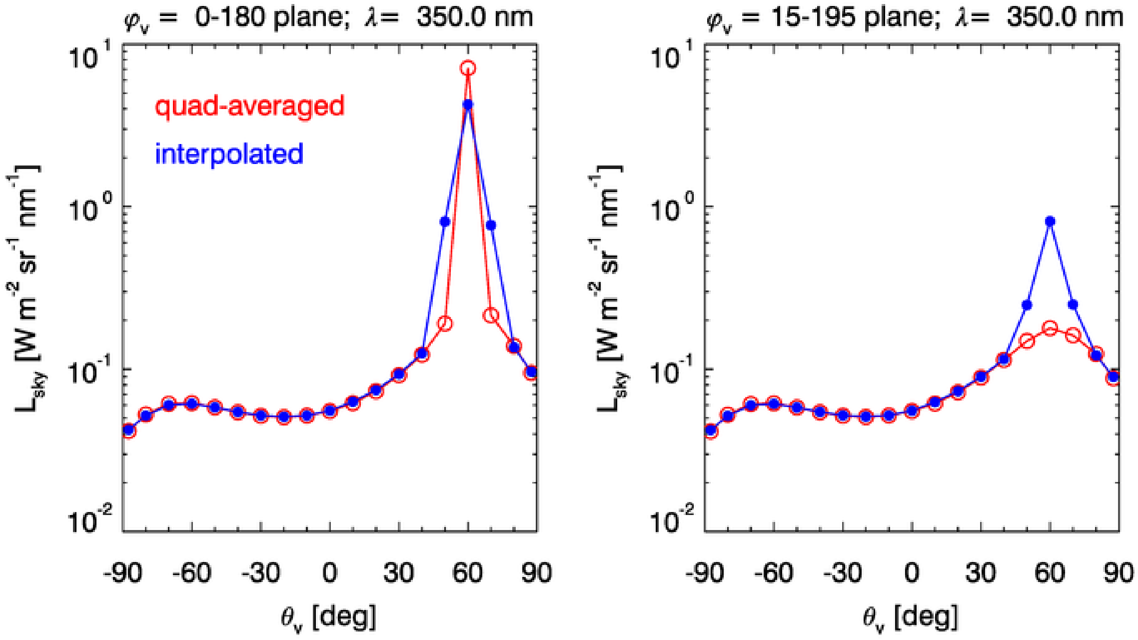

Figure 3: Quad-averaged sky radiances obtained from the same input file. The red symbols are the data taken as quad averages. The blue dots are the same data used for interpolation to compute quad averages. The left panel is values in the ϕ = 0-180 plane of the sun; the right panel is values in the ϕ = 15-195 deg plane.

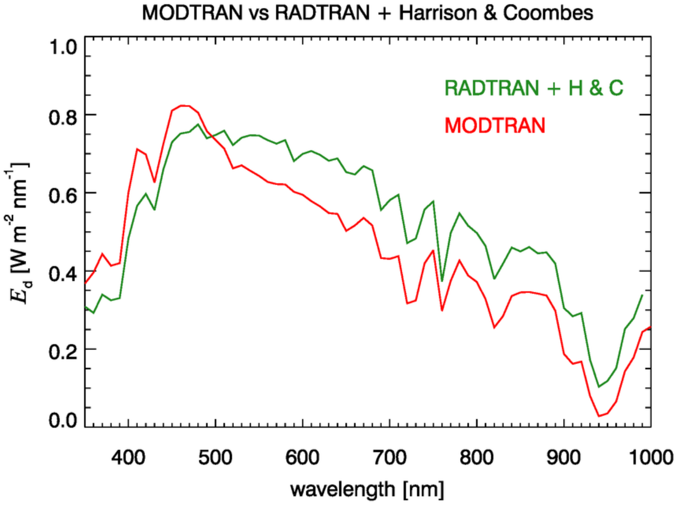

Figure 4: Total sky irradiances $E_d(\lambda)$ computed by RADTRAN and MODTRAN for a 60 deg solar zenith angle and roughly similar atmospheres.

Figure 5 shows radiances in the solar plane at depth $z = 0$ (just below the mean sea surface) and wavelength $\lambda = 500$ nm, where the irradiances differ by less than 2%. The IOPs were obtained using the "New Case 1" IOP model in HydroLight, with a chlorophyll value of 5 mg m^{-3}. The water was infinitely deep, homogeneous, and inelastic effects (Raman scattering by the water, and chlorophyll and CDOM fluorescense) were included. The resulting differences are due almost entirely to the differences in the shapes of the radiance distributions. In HydroLight, angles (θ, ϕ) give the direction of photon travel. Thus in this figure, $\theta = 0$ is downwelling radiance that would be seen looking at the zenith; $\theta = \pm 180$ is upwelling radiance seen looking at the nadir. The red circles are the in-water radiances using the MODTRAN sky data as quad averages. The blue dots are the same data used as quad center values, with interpolation done as described above to compute the quad averages. These two MODTRAN-based radiances are very nearly the same except in the directions of the solar quad and the adjacent quads, where the differences seen in Fig. 3 carry though to the underwater radiances. The green dots are the radiance computed using the RADTRAN-X and Harrison and Coombes models. There is a significant difference in the MODTRAN vs RADTRAN+H&C downwelling radiance distributions ($-90 < \theta < +90$) at some angles, owing to the difference in the shapes of the radiance distributions as was seen in the right panel of Fig. 1.

However, the upwelling radiance distributions are very similar for the three simulations. The nadir-viewing radiances differ by only 0.6%, which is comparable to the differences in the irradiances. (Note that the magnitudes at one wavelength are somewhat affected by inelastically scattered light from shorter wavelengths.) The differences in the downwelling radiances disappear with depth as scattering re-orients the radiance entering the water from the air. Figure 6 shows the radiances at 5 m depth. Of course, as the depth increases further, all radiances approach the shape of the asymptotic radiance distribution, which is determined solely by the IOPs.

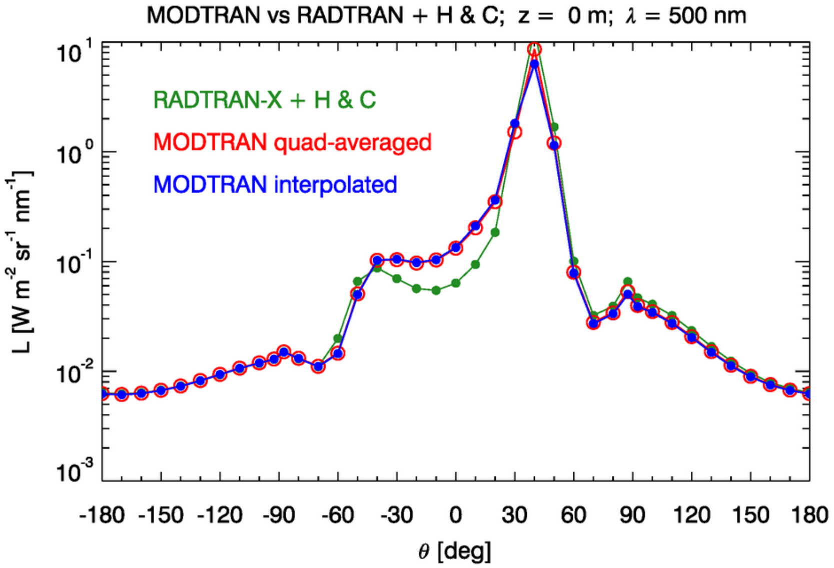

Figure 5: Radiance distributions at 500 nm just beneath the sea surface for MODTRAN vs RADTRAN + Harrison and Coombes sky radiance models.

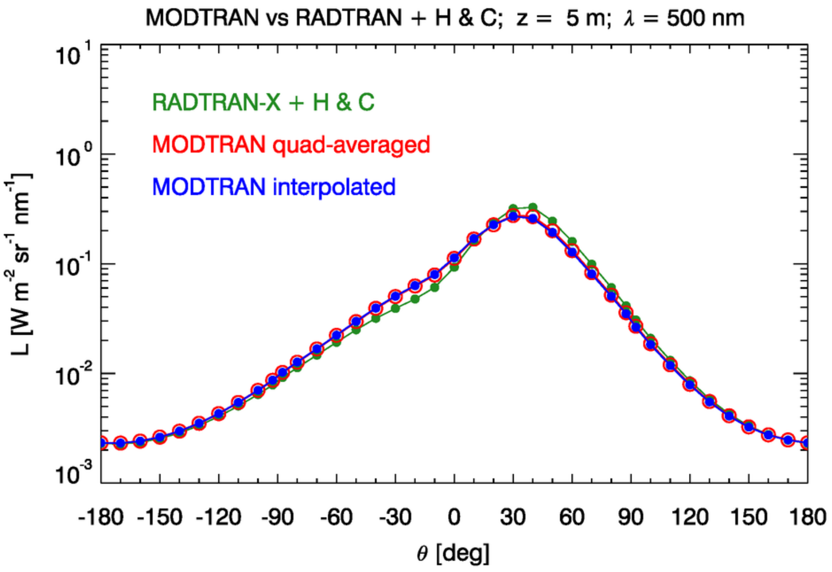

Figure 6: Same as Fig. 5, but at a depth of 5 m.

The small difference in the nadir-viewing radiances have a negligible effect the remote-sensing reflectance $R_{\rm rs}$, as seen in Fig. 7. For AOPs like $R_{\rm rs}$ or $K_{\rm d}$, the magnitude differences in the incident irradiances divide out. The $R_{\rm rs}$ spectra differ by less than 1% except in the chlorophyll fluorescence band, where there is a difference of up to 10% caused by the differences in irradiance at shorter wavelengths being re-emitted in the fluorescence band.

Warning on Runs with $\lambda < 300$ or $\lambda >$ 1000 nm

As mentioned previously, the use of a user-defined sky radiance frees HydroLight from the wavelength constraints of the RADTRAN-X sky irradiance model. However, a run requires that the IOPs, and perhaps other quantities such as bottom reflectances, be defined at all wavelengths requested in the run. In HydroLight, if values are not defined at the requested depth or wavelength, values at the nearest depth or wavelength will be used. Most of the databases that come with HydroLight define IOPs, bottom reflectances, etc. over only the $300 \leq \lambda \leq 1000$ nm wavelength range. The exception is the file of pure-water absorption and scattering coefficients, which covers 200 to 2000 nm. The reason that, at least in version 5.3, the databases have not been updated for wavelengths outside the 300-1000 range is that almost no data or models are available for these quantities. That is to say, the absorption and scattering coefficients of phytoplankton, mineral particles, etc. are simply not known for $\lambda < 300$ nm or $\lambda > 1000$ nm. Many of the original models and measurements used to define the IOPs for 300-1000 nm are really valid only for 400-700 nm, and in many cases extrapolation those values down to 300 nm and up to 1000 nm is quite uncertain. Extrapolating further would be totally unjustified.

Thus, if a run is made from 350 to 1500 nm, the IOPs other than water will be available only up to 1000 nm. Beyond 1000 nm, the correct IOPs for the pure water component will be used, but other IOPs (and perhaps bottom reflectance, etc.) will have their values at 1000 nm. The

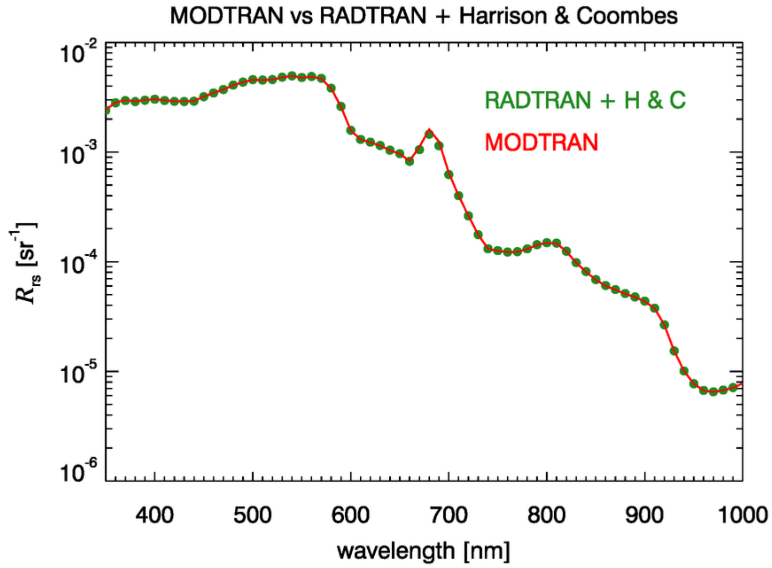

Figure 7: Remote-sensing reflectances $R_{\rm rs}$ corresponding to Fig. 5.

consequence of this is shown in Fig. 8. That figure used the MODTRAN sky radiances from 350 to 1500 nm, some of which were seen in Fig. 1. The IOPs were the same as in Figs. 5-7, namely Case 1 water with $Chl = 5$ mg m^{-3}. The RADTRAN and MODTRAN Case 1 curves are the same as plotted in Fig. 7. The IOPs for the MODTRAN Case 1 run above 1000 nm are as follows:

- The pure water absorption and scattering coefficients for sea water are used. The water absorption coefficient at 1000 nm is $a_w = 37.697$ m^{-1} and the sea water scattering coefficient is $b_w = 0.0001$ m^{-1}. The water absorption reaches a value of $a_w = 1875.8$ m^{-1} at 1500 nm, and b_w decreases to almost zero.

- The Case 1 IOPs for phytoplankton have their values at 1000 nm: The phytoplankton absorption is $a_{\rm ph} = 0$, but $b_{\rm ph} = 1.4274$ m^{-1}. Those values are added to the water values at all wavelengths greater than 1000 nm to get the total IOPs.

Thus the total absorption coefficient beyond 1000 nm is that of pure water because the phytoplankton absorption is 0, but the total scattering coefficient is that of phytoplankton, 1.4274 m^{-1}, because the water scattering is negligible. This is not a physically realistic set of IOPs.

A run was made for pure water, which gives the curve shown in blue. Beyond 1000 nm, this spectrum closely parallels the shape of the MODTRAN run for $Chl = 5$ mg m^{-3}, but the $Chl = 5$ curve is offset above the pure-water curve by two orders of magnitude because of the presence of the constant scattering coefficient, as just discussed.

It is also noted that the MODTRAN curves in Fig. 8 show a peculiarity between 1360 and 1390 nm. This occurs because the atmosphere is essentially opaque in that region because of strong absorption by water vapor. Figure 9 shows that the irradiance reaching the surface is of order 10^{-9} of that at visible wavelengths, as computed by MODTRAN. These very small irradiances cause numerical inaccuracies in the MODTRAN radiances, which result in bad values for $R_{\rm rs}$ in this absorption band.

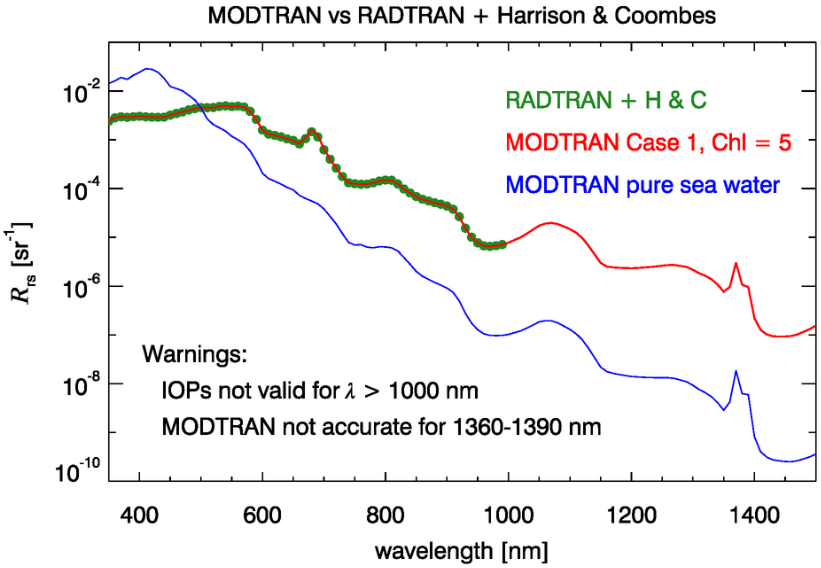

Figure 8: Remote-sensing reflectances R_{rs} for Case 1 water with $Chl = 5$ mg m^{-3} below 1000 nm, but with unphysical IOPs above 1000 nm (red curve). The blue curve is R_{rs} for pure sea water.

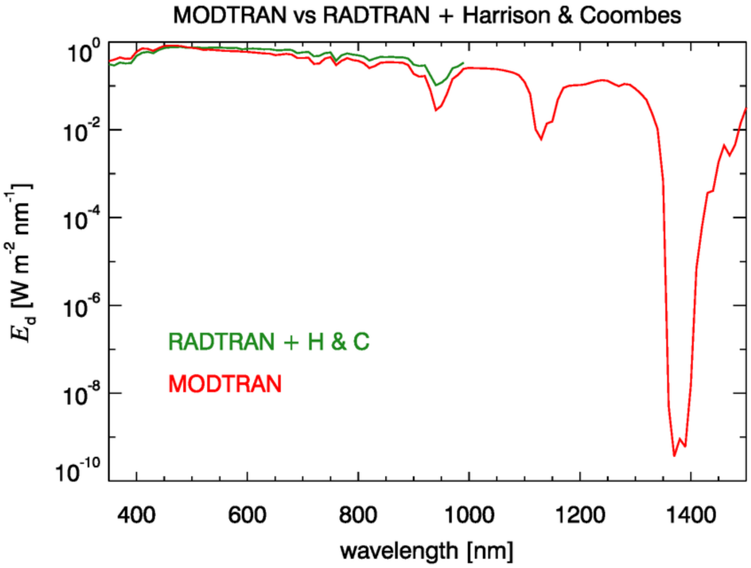

Figure 9: Incident sky irradiances showing the effect of the atmospheric absorption band between 1360 and 1390 nm.

Thus the use of user-supplied sky radiances does allow HydroLight to be run outside the 300-1000 nm range. However, the results are likely to be in error because of incorrect IOPs when HydroLight's currently available IOP models are used. *The user who wants to run HydroLight outside the 300-1000 range must first define all IOPs and other needed quantities before making the run. The best way to do this is to input files of measured IOPs using the "Measured IOPs" option in the user interface.* When measured IOPs are used, the IOP bio-geo-optical models with their limited-wavelength-range databases are not used.

Finally, because of the large water absorption values in the IR, it makes no sense to do a HydroLight run to large depths at those wavelengths. In the runs shown above, the runs were made to 10 m depth at all wavelengths. At 1500 nm, the value of $a_w = 1875.8 \text{ m}^{-1}$ means that 10 m is almost 19,000 optical depths. Consequently, the runs took over one hour, even though the RTE solution was only a couple of seconds per wavelength at blue and green wavelengths.

References

A. Berk, G. P. Anderson, P. K. Acharya, J. H. Chetwynd, L. S. Bernstein, E. P. Shettle, M. W. Matthew, and S. M. Adler-Golden. *MODTRAN4 Users Manual.* Air Force Research Lab., Space Vehicles Directorate, Hanscom AFB, MA, 2000.

W. W. Gregg and K. L. Carder. A simple spectral solar irradiance model for cloudless maritime atmospheres. *Limnol. Oceanogr.*, 35:1657–1675, 1990.

A. W. Harrison and C. A. Coombes. An opaque cloud cover model of sky short wavelength radiance. *Solar Energy*, 41:387–392, 1988.

F. Kasten and G. Czeplak. Solar and terrestrial radiation dependent on the amount and type of cloud. *Solar Energy*, 24:177–189, 1980.

C. D. Mobley. *Light and Water: Radiative Transfer in Natural Waters.* Academic Press, 1994.